ACS APPLIED MATERIALS & INTERFACES

Research Article

www.acsami.org

Fast-Response Room Temperature Hydrogen Gas Sensors Using Platinum-Coated Spin-Capable Carbon Nanotubes

Daewoong Jung,* Maeum Han, and Gil S. Lee

Department of Electrical Engineering, University of Texas at Dallas, 800 West Campbell Road, Richardson, Texas 75080-3021, United States

ABSTRACT: We report the properties of a hydrogen (H_2) gas sensor based on platinum (Pt)-coated carbon nanotubes (CNTs) in this paper. To fabricate the Pt−CNT composite sensor, a highly aligned CNT sheet was prepared on a glass substrate from a spin-capable CNT forest, followed by electrobeam (e-beam) deposition of Pt layers onto the CNT sheet. To investigate the effect of Pt on the response of the sensor, Pt layers of different thicknesses were deposited on the CNT sheets. A Pt thickness of 6 nm yielded the highest response for H_2 detection, whereas Pt layers thinner or thicker than 6 nm led to a reduction of the surface area for gas adsorption and, consequently, decreased response. The Pt−CNT composite sensor detects H_2 concentrations of 3−33% at room temperature and shows reproducible behavior with fast response and recovery times.

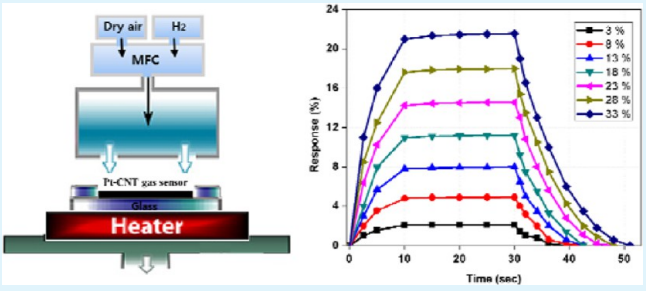

KEYWORDS: *spin-capable carbon nanotube, hydrogen sensor, spillover, activation energy, chemical sensitization platinum*

1. INTRODUCTION

Considerable research has been focused on the development of hydrogen (H_2)-based energy storage to overcome environmental problems associated with fossil energy sources, such as air pollution, global warming, and exhaustion of the Earth's resources.[1] H_2 is a clean, efficient, and renewable energy source that will be extensively used in the future for power generation and in the automotive and energy-storage industries. However, safety issues involving H_2 gas such as a wide explosive concentration range (4−75%), low ignition energy (0.02 mJ), and high flame propagation velocity are major challenges in the development of H_2-based applications. Moreover, the human senses do not detect H_2 gas because it is colorless, odorless, and tasteless.[1,2] Therefore, early detection of H_2 leakage and accurate monitoring are very important in ensuring safety at H_2-based facilities.

Diverse chemical sensors have been reported and are typically classified into eight types according to the sensing mechanism:[3] catalytic, thermal-conductivity-based, electrochemical-resistance-based, work-function-based, mechanical, optical, and acoustic. Recently, resistance-based sensors have been widely used for gas sensors because of their straightforward measurement principle (resistance change), simple structure, and low-cost fabrication process for commercialization.[3−5] Resistance-based sensors have been developed using semiconducting metal oxides that normally operate at elevated temperatures. This requires high power consumption and creates an elevated risk of explosion. Consequently, there has been extensive research on sensing materials for gas detection that operate at lower temperatures.[6,7]

Over the past decade, carbon nanotube (CNT)-based gas sensors have been extensively investigated for real-time chemical sensor applications in monitoring and detecting many gases of interest in environmental pollution, chemical processes, and medical fields.[8] Unlike classical semiconducting metal oxide gas sensors requiring high operating temperatures (>300 °C), CNT-based gas sensors are capable of room temperature detection of hazardous gases such as ammonia (NH_3) and nitrogen dioxide (NO_2).[9] It is well-known that adsorption/desorption of electron-donating or -withdrawing gas molecules on the CNT surface can transfer electrons because of the difference in the electronic potential between the two materials. This process causes a change in the resistance of the CNT, which is measured as the sensor's response.[9,10] However, prior works have demonstrated that CNT-based gas sensors do not detect H_2 at room temperature because of both weak adsorption and high activation energy in the interaction between H_2 molecules and CNT.[11,12]

To improve the room-temperature-sensing performance, great effort has been devoted to CNT-based gas sensors. For instance, appropriate post-treatments of the CNTs by chemical modification or ultraviolet (UV) treatment improved the performance of gas sensors.[13−15] In particular, thermal annealing not only leads to high gas response and fast response time but also alleviates recovery issues if the resistance of a CNT-based gas sensor does not return to its initial values during desorption.[16,17]

Received: September 24, 2014
Accepted: January 26, 2015
Published: January 26, 2015

DOI: 10.1021/am506578j
ACS Appl. Mater. Interfaces 2015, 7, 3050−3057

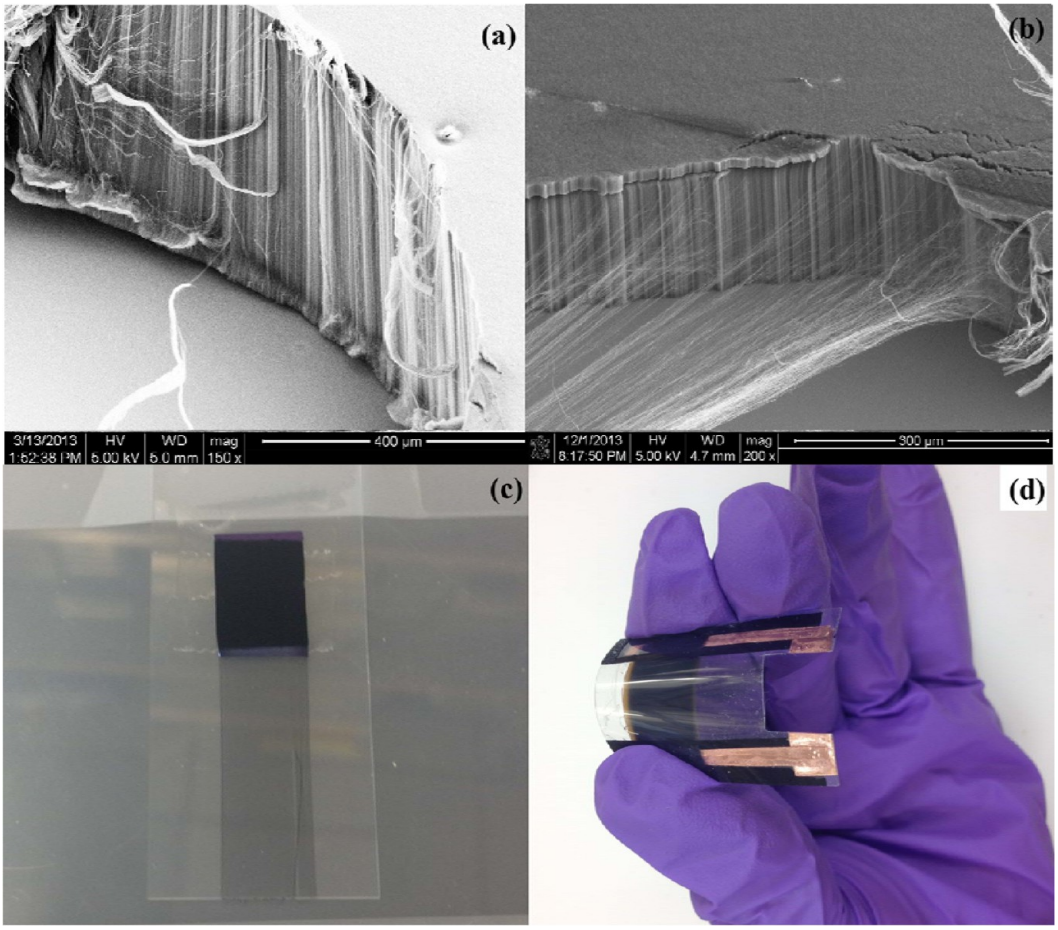

Figure 1. SEM images and pictures of (a) a spin-capable CNT forest, (b and c) CNT sheets pulled from the CNT forest, and (d) a fabricated sensor.

Besides post-treatments, synthesizing CNTs coated with various dopants, either noble metals or metal oxides, stands out as a promising alternative approach that shows enhanced response and selectivity to different gases. These properties result from the catalytic activity of noble metals[18−21] or the formation of a p−n junction between semiconducting metal oxides and the CNT.[22,23] Notably, noble metals such as gold (Au), platinum (Pt), and palladium (Pd) are extensively used to enhance the detection of specific gases. It is well-known that Pt is a stable and effective catalyst that can significantly increase the reaction capability for H_2 molecules by chemical sensitization via a "spillover" effect.[10,20,21,24−27] It can be effectively employed to enhance the response and selectivity as well as to provide fast response and recovery times.

Although previous studies demonstrated high-performance H_2 sensors based on Pt−CNT hybrid composites,[28,29] there has been little research reported on the detection of H_2 gas using highly aligned and uniformly distributed CNT sheets.[30,31] The use of highly aligned CNT, namely, spin-capable CNT, has been greatly beneficial for carrier transport during the adsorption/desorption process and for providing a large surface area of CNT.[32−34] In addition, high density and large contact area between individual CNTs helps to maximize access to individual CNTs and provide stable electrical contacts for a Pt−CNT composite. Because it is the basic platform in the sensor structure, the incorporation of uniformly distributed CNTs into the sensor is a highly critical step to achieve repeatable and reliable performance of the sensor.[35] Therefore, the use of highly aligned, well-distributed CNTs is an important factor in determining the response of CNT-based sensors.

In order to use an as-grown CNT forest as a sensor platform, the CNT forest must be transferred from an initial substrate (usually silicon) to the main sensor's body. There are several techniques to manipulate the CNTs, such as filtration, dielectrophoresis, spraying, inkjet printing, and dry spinning for the transfer, separation, alignment, and positioning of CNT into the main body.[36−39] Researchers have selected among these preparation processes by considering the advantages and disadvantages for their own applications. Among these fabrication methods, the dry-spinning technique holds more advantages because it uses a spin-capable CNT. This is a special kind of vertically aligned CNT forest having a higher surface density and better alignment of CNTs than the ordinary form.[40−42] The spin-capable CNTs stand straight and have few defects in their structure. This improved directional alignment and smaller number of defects with spin-capable CNTs in sensors has led to better performance than with nonaligned, randomly distributed CNTs.

In this study, a comparison between Pt−CNT and CNT sensors examined the effect of Pt layers on their performance. The experimental results show that the Pt−CNT sensor is more sensitive to H_2 gas at room temperature, with a faster response time, than the CNT sensor. We further investigated possible sensing mechanisms and the effect of recovery issues after exposure to 3−33% of H_2 in air.

DOI: 10.1021/am506578j
ACS Appl. Mater. Interfaces 2015, 7, 3050−3057

2. EXPERIMENTAL DETAILS

2.1. Sensor Fabrication. Our previous experiments produced transparent conductive CNT sheets by using a simple CNT spinning method.[43−45] A 5−6-nm-thick iron film was deposited on a 330-μm-thick p-type silicon wafer using electrobeam (e-beam) evaporation. The thickness was monitored by a quartz-crystal sensor fixed inside the e-beam evaporation chamber. Catalyst annealing and CNT growth were performed in a vertical-cylinder chamber at atmospheric pressure. Flow rates of helium (He; 5 slm), C_2H_2 (100 sccm), and H_2 (100 sccm) were controlled by electronic mass-flow controllers (MFCs). After purging with He for 10 min, the chamber was heated to 780 °C within 15 min (ramping rate: 50 °C/min), after which the growth of CNTs was carried out at 780 °C by adding acetylene gas to the flow for 5 min. Then, the C_2H_2 and H_2 gas flows were ended, and the sample was rapidly cooled. As shown in Figure 1, a superaligned CNT film is continuously drawn from the CNT forest. The dimension of the sensor was 1.2 × 1.7 cm^2, and copper tape was attached at either end of the CNT sheet on the substrate in order to be used as an electrode. Specimens were fabricated by depositing different thicknesses of Pt layers, using e-beam evaporation, having various thicknesses from 2 to 8 nm over the entire surface of the CNTs.

2.2. Sensor Measurements. The sensing measurements were conducted in a conventional gas-flow apparatus, consisting of a chamber with separated gas inlet and outlet. Air and H_2 were used as the carrier and test gases, respectively. The two gases arriving from separate lines were mixed and fed into the chamber through the gas-inlet line. MFCs were used to control the flow rates of air and H_2, and the flow rate of the gas mixture was set to 100 sccm. The variation in the electrical resistance of the sensors with time and concentration was measured by a Keithley 2400 sourcemeter.

3. RESULTS AND DISCUSSION

3.1. Gas-Sensing Properties. The CNT with 6 nm Pt thickness and CNT sensors were placed in the gas-flow chamber and exposed to a 3−33% H_2 gas-in-air atmosphere at room temperature. The percentage response change was defined from the resistance difference before and after adsorption of H_2 molecules, divided by the initial resistance in air. The response equation is

$$\text{response}\ (\%) = [(R - R_0)/R_0] \times 100 \qquad (1)$$

where R and R_0 are the sensor resistances upon exposure to the H_2−air mixture and air, respectively. Figure 2 shows the responses of the CNT sensors with and without Pt at room temperature. It is clear that the electrical resistance of both sensors increases with the introduction of H_2 gas, and higher concentrations of H_2 gas further increase the electrical resistance of the sensors; however, the Pt−CNT sensor exhibits much higher response compared to the CNT sensor. As expected, the CNT sensor without Pt shows much lower response at room temperature, owing to the large activation energy and poor adsorption of H_2 molecules.[11,12,33,34]

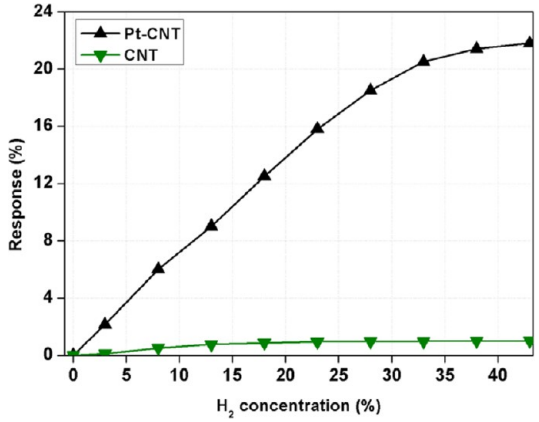

Figure 2. Response of the gas sensor as a function of the H_2 concentrations, showing the effect of the addition of Pt layers.

The enhanced H_2 gas response of Pt−CNT is strongly related to chemical sensitization via a "spillover" effect at the surface of the Pt layers, producing dissociation of gas molecules (e.g., H_2) into gas atoms (H^+), with the reaction occurring even at room temperature.[21,24,46,47] The resulting H^+ atom dissolves readily into a Pt layer, lowering its work function, which, in turn, results in electron transfer from the Pt layer to the CNT. In the case of electron-withdrawing-induced catalytic spillover (e.g., oxidizing gases, O_2, NO, NO_2), the energy levels are likely acceptor-gap states, while for electron-donating-induced spill-over (e.g., reducing gases, H_2, NH_3, CO), these energy levels are likely donor-gap states. In the acceptor-gap states, electrons can move from p-type CNTs to the energy states and the number of majority carriers (holes) is increased, leading to decreased resistance of the CNTs. In the donor-gap states, on the other hand, electrons can be transferred from the energy state to a conduction band of the p-type CNT, followed by recombination between majority hole carriers and transferred electrons, decreasing the free net (hole) charge density.[46,47] This process results in increased resistance of the CNTs. These sensing mechanisms were proposed by Kong et al.[48] Our results are therefore in agreement with prior work.[28,29,46,47]

The response time is usually defined as the time to reach 90% of the total change of the electrical resistance upon exposure to gas. As shown in Figure 3, a fast response time of

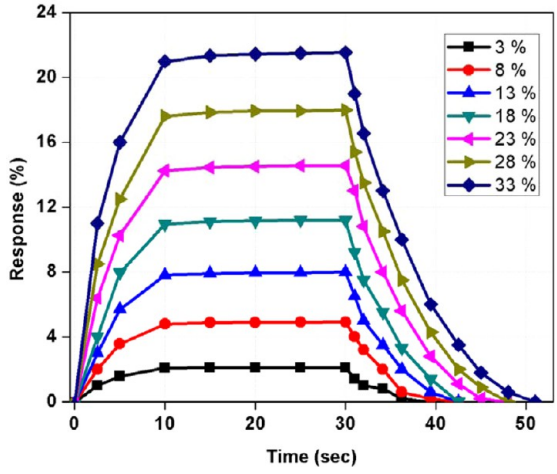

Figure 3. Response of the gas sensor with Pt−CNT as a function of time with respect to H_2 concentrations.

~10 s was measured when H_2 was injected, with an instantaneous decay (20 s) in the resistance after its removal. These measured response and recovery times are much faster than those of previously reported metal-oxide-based gas sensors (a few minutes).[49−53] The Pt−CNT sensor also shows higher response compared with prior works.[50−53] The fast response and recovery times resulted from highly conductive CNTs being used as the basic supporting body as well as from the superior catalytic effect of Pt layers. Dang and co-workers reported that the added CNT acts as a conducting wire and increases the electrical conductivity of the sensing materials, in

DOI: 10.1021/am506578j
ACS Appl. Mater. Interfaces 2015, 7, 3050−3057

which the CNT composites have a one-dimensional nature.[54,55] The CNTs play a role as both a carrier collector and a conducting channel in the sensor, and Pt layers have high solubility for the H^+ atoms, giving both rapid charge migration and high response. Moreover, a Pt−CNT sensor with a wide range of gas detections (1−45%) can be commercially utilized because H_2 concentrations in excess of 4% under ordinary atmospheric conditions become potentially explosive.[56−59]

In addition, it is well-known that the alignment, surface area, distribution, and density of CNTs greatly influence the performance of CNT-based sensors.[35,60] A CNT sensor is fabricated by putting together hundreds of thousands of individual CNTs, and their assembly in the sensor is sustained by van der Waals forces.[61,62] The surface morphology of a CNT sensor is highly dependent on the density of the as-grown CNT forest, the transfer method, and defects of the CNTs, which can influence electrical charge transport during the sensing process.[40−42] Therefore, the alignment, surface area, distribution, and density of CNTs are critical factors in determining the response of a CNT-based sensor.

In order to investigate the effect of the surface morphology on the CNT sensor performance, two sensors were fabricated using different methods for transferring the CNTs to the substrates. The two methods were dry spinning and imprinting (after that, 6 nm Pt layers were deposited on both CNT films); SEM images of dry-spun and imprinted CNT films show different surface morphologies. Figure 4a shows that the dry-spun CNT film exhibits a highly ordered alignment and uniform distribution. On the other hand, the imprinted film in Figure 4b shows random disorder and poorly aligned CNTs. As seen in Figure 4c, much higher response was observed with a dry-spun CNT film than an imprinted film (35 and 60 s for response and recovery times, respectively). The increased response was due to the fact that a dry-spun CNT offered larger surface area for gas adsorption and its uniformly aligned parallel CNTs served as a highly conductive electron pathway during the sensing process. In other words, the large surface area, aligned CNTs, and uniform distribution in the sensor result in efficient electron percolation between the Pt−CNT and H_2 molecules, thereby improving the sensor performance.[35]

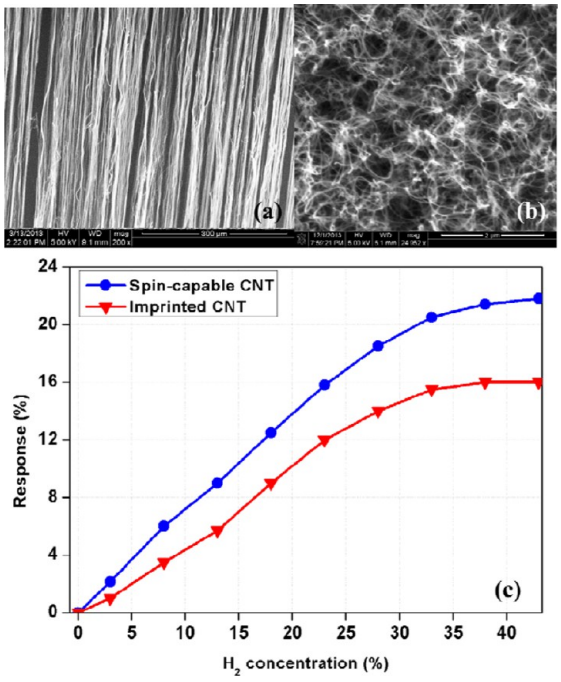

Figure 4. Surface morphologies of (a) dry-spun and (b) imprinted CNT films. Also shown are (c) responses of the sensors against the H_2 concentration.

In addition, further experiments were conducted to investigate the correlation of the structural morphology with a sensor's response. Four types of samples fabricated with different thicknesses of Pt layers (2, 4, 6, and 8 nm) were prepared on the surface of a CNT sheet using e-beam evaporation (Figure 5). The thickness was controlled by a quartz-crystal sensor fixed inside the e-beam evaporation chamber. The response of the sensors in terms of different loading of Pt layers is plotted versus the H_2 concentration in Figure 6. The response increases with increasing thickness, up to 6 nm. However, the response decreased for thickness further increased to 8 nm.

Two mechanisms, structure and catalytic effects, can be used to interpret this enhancement. First, thicker Pt layers (up to 6 nm) result in increasing surface area for the interaction between Pt−CNT and H_2 molecules, providing more active sites and facilitating gas diffusion (called the "structure effect"), which could enhance the response of the sensor.[22,33,34] Therefore, increased surface area of Pt on the CNT sheet is the first main reason for this improvement. Second, the outermost Pt atoms on the surface of the Pt layer are expected to have more catalytic behavior because of their low activation energy; this behavior increases stepwise with increasing Pt layers, eventually reaching its peak at an optimal layer thickness.[46,47] Penza et al. mentioned that the activation energy (energy levels of the gap states) between the Pt−CNT and gas molecules depends on the catalyst used, its particle size, and molecular fragments dissolved.[60] Rothschild and Komem also discussed the effect of the grain size on the response of nanocrystalline metal oxide gas sensors and found that the response of the gas sensor was greatly influenced by the size of the nanocrystals.[63] In our case, 6 nm of Pt layers on the CNT film shows the most active catalytic behavior. Therefore, the surface and structural morphologies of sensing materials have a significant effect on their catalytic properties and on the response of the Pt−CNT sensor.

On the other hand, recovery is a main issue for CNT-based sensors, in the loss of its initial resistance value and the long time returning to the initial resistance after gas flow ends.[64−66] However, it was observed that the resistance of the sensor completely returned to its initial value during desorption, without any additional treatment (Figure 3). This result is likely related to the interactions between the Pt layers on CNTs and gas molecules. The recovery of the gas sensor mainly involves three steps: desorption and diffusion of the target gas from the surface of the sensing material, readsorption of oxygen from air, and dissociation of oxygen at the surface of the sensing material.[22,46] These steps might be highly affected by the surface morphology of the sensing material. As mentioned, upon exposure to H_2, Pt layers initially absorb the H_2 molecules on their surface, a process known as molecular physisorption, and then H_2 molecules are separated into H^+ atoms at the outer surface of the Pt layers, a process known as molecular chemisorption. Without Pt layers in the sensor configuration, the activation energy between the CNTs and H_2 molecules is large, requiring higher energy and/or a longer time to detach from the CNTs. Some researchers have made efforts to

DOI: 10.1021/am506578j
ACS Appl. Mater. Interfaces 2015, 7, 3050−3057

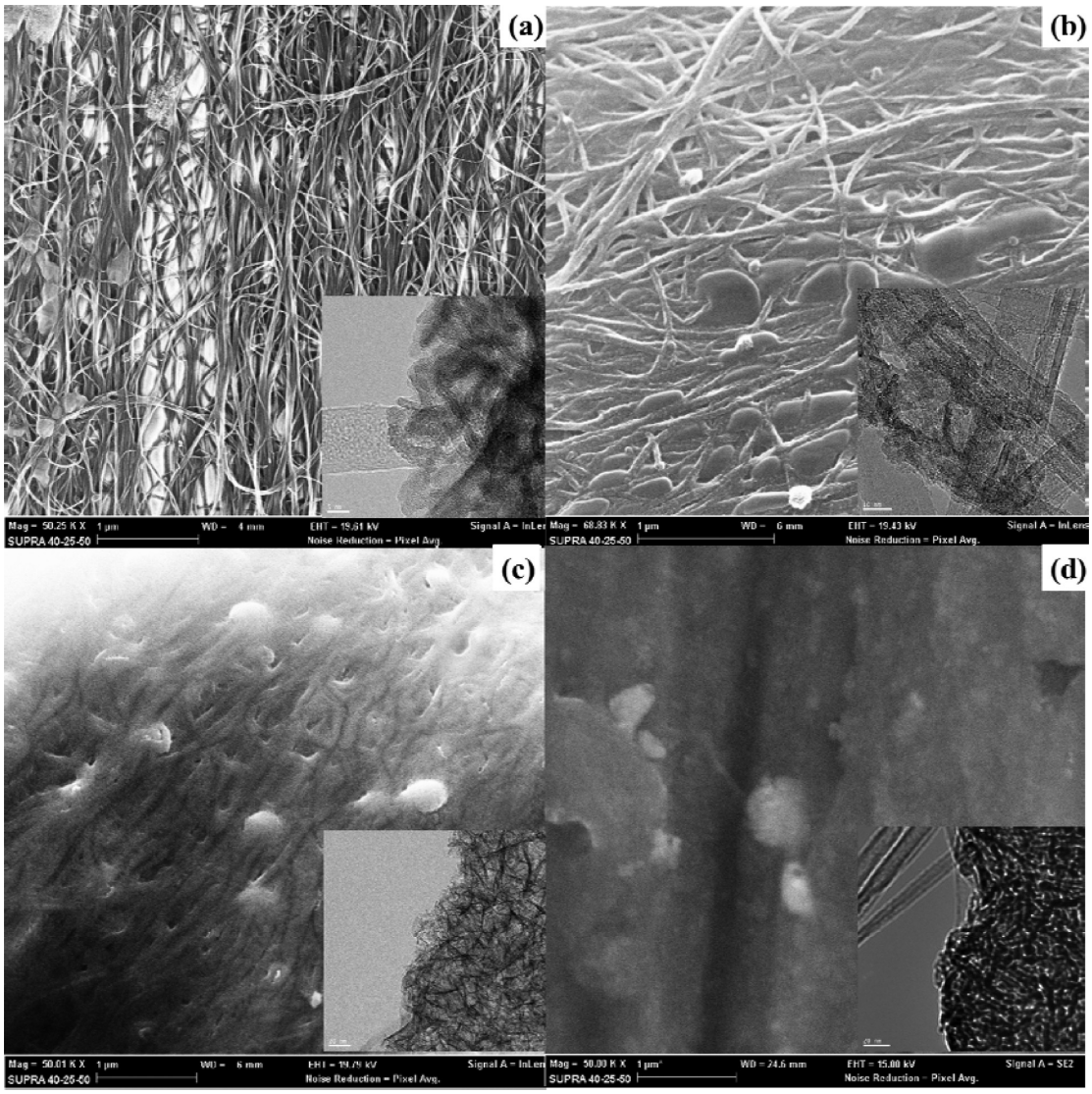

Figure 5. Surface morphology and microstructure of the gas sensor with Pt−CNT. SEM and TEM (inset) images of Pt composites deposited for (a) 2, (b) 4, (c) 6, and (d) 8 nm.

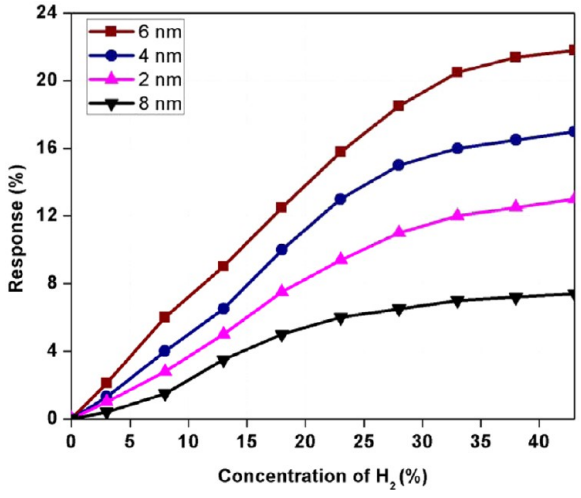

Figure 6. Responses of Pt−CNT composites as a function of the H_2 concentration for different Pt thicknesses.

accelerate the recovery response of CNT sensors by lowering the activation energy by means such as UV-light-induced photodesorption or with high-vacuum conditions.[67−69] Pt is a well-known electrocatalyst for splitting off H^+ atoms and has lower activation energy for H_2 compared to CNTs, facilitating desorption of H_2 molecules even at room temperature.

The repeatability and reliability of sensors are two important factors for evaluating the performance, especially for CNT-based sensors, because they often exhibit response variation under test cycling due to modification of their surface morphology. As mentioned, many CNT-based sensors exhibit imperfect recovery to their initial resistance after the flow of H_2 ends. The response fluctuation may be related to irreversible deterioration of the CNT structure or redistribution of CNTs because of their low density in the sensor. The performance of a commercially viable sensor should be repeatable and reliable.[70] In order to examine the repeatability and reliability of the Pt−CNT sensor, multiple tests were performed at 23% H_2 concentration. Figure 7 demonstrated that repeatable and reliable behaviors were observed, with only minor hysteresis. This repeatability of the sensor was attributed to strong

DOI: 10.1021/am506578j
ACS Appl. Mater. Interfaces 2015, 7, 3050−3057

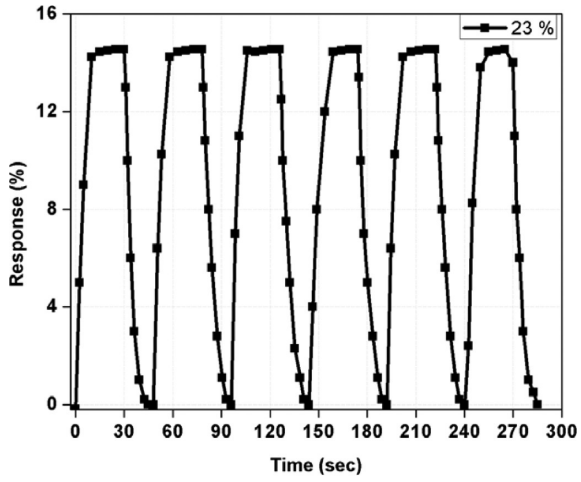

Figure 7. Response of the 6 nm Pt−CNT composite under repeated tests (23% H_2 in air).

interaction between the CNT film and Pt layers, which provides stable electrical contacts for the composites.

4. CONCLUSION

In summary, Pt−CNT composite sensors for H_2 gas sensing have been prepared using spin-capable CNT, coated with Pt layers as a highly sensitive noble metal. Decoration of the CNT film with Pt layers, prepared by an e-beam process, significantly enhanced the gas response at room temperature. The gas response of the Pt−CNT sensors depended on the thickness of the Pt coating layer, which was studied in the range 2−8 nm. The highest response to H_2 gas was found for a CNT film decorated with 6 nm of Pt nanoparticles, and much-reduced response was measured with a CNT sensor without Pt layers. Structural and catalytic mechanisms were suggested to explain the enhanced response of the Pt−CNT sensor over the CNT sensor. A comparison of the sensors fabricated with spin-coated and imprinted CNTs shows that highly ordered CNTs and uniformly distributed CNT films are beneficial for electrical charge transport during the sensing process. This Pt−CNT sensor can be a very useful gas sensor with high response, repeatability, and reliability for monitoring H_2 leakage in H_2-based facilities.

AUTHOR INFORMATION

Corresponding Author

*E-mail: dwjung@utdallas.edu.

Notes

The authors declare no competing financial interest.

REFERENCES

(1) Buttner, W. J.; Post, M. B.; Burgess, R.; Rivkin, C. An Overview of Hydrogen Safety Sensors and Requirements. *Int. J. Hydrogen Energy* **2011**, *36*, 2462−2470.

(2) Jung, D.; Han, M.; Lee, G. S. Room Temperature Gas Sensor Using Carbon Nanotube with Cobalt Oxides. *Sens. Actuators, B* **2014**, *204*, 596−601.

(3) Hubert, T.; Boon-Brett, L.; Black, G.; Banach, U. Hydrogen Sensor-Review. *Sens. Actuators, B* **2011**, *157*, 329−352.

(4) Li, X.; Gu, Z.; Cho, J.; Sun, H.; Kurup, P. Tin−copper Mixed Metal Oxide Nanowires: Synthesis and Sensor Response to Chemical Vapors. *Sens. Actuators, B* **2011**, *158*, 199−207.

(5) Lu, C.; Chen, Z.; Singh, V. Highly Hydrogen-sensitive SnO_2 Nanoscale-particle Films with Platinum Electrodes. *Sens. Actuators, B* **2010**, *146*, 145−153.

(6) Hassan, J. J.; Mahdi, M. A.; Chin, C. W.; Abu-Hassan, H.; Hassan, Z. Room-temperature Hydrogen Gas Sensor with ZnO Nanorod Arrays Grown on Quartz Substrate. *Phys. E* **2012**, *46*, 254−258.

(7) Hu, M.; Jia, D. L.; Liu, Q. L.; Li, M. D.; Sun, P. Effects of Rapid Thermal Annealing on the Room-temperature NO_2-sensing Properties of WO3 Thin Films under LED Radiation. *Chin. Phys. B* **2013**, *22*, 068204.

(8) Zhang, T.; Mubeen, S.; Myung, N. V.; Deshusses, M. A. Recent Progress in Carbon Nanotube-based Gas Sensors. *Nanotechnology* **2008**, *19*, 332001.

(9) Valentini, L.; Armentano, L.; Kenny, J. M.; Cantalini, C.; Lozzi, L.; Santucci, S. Sensors for Sub-ppm NO_2 Gas Detection Based on Carbon Nanotube Thin Films. *Appl. Phys. Lett.* **2003**, *82*, 961−963.

(10) Wang, Y.; Yeow, J. T. W. A Review of Carbon Nanotube-based Gas Sensors. *J. Sens.* **2009**, *2009*, 493904.

(11) Mubeen, S.; Zhang, T.; Yoo, B.; Deshusses, M. A.; Myung, N. Y. Palladium Nanoparticles Decorated Single-walled Carbon Nanotube Hydrogen Sensor. *J. Phys. Chem. C* **2007**, *111*, 6321−6327.

(12) Zilli, D.; Bonelli, P. R.; Cukierman, A. L. Room Temperature Hydrogen Gas Sensor Nanocomposite Based on Pd-decorated Multi-walled Carbon Nanotubes Thin Films. *Sens. Actuators, B* **2011**, *157*, 169−176.

(13) Dhall, S.; Jaggi, N.; Nathawat, R. Functionalized Multiwalled Carbon Nanotubes Based Hydrogen Gas Sensor. *Sens. Actuators, A* **2013**, *201*, 321−327.

(14) Kim, D.; Pikhitsa, P. V.; Yang, H.; Choi, M. Room Temperature CO and H_2 Sensing with Carbon Nanoparticles. *Nanotechnology* **2011**, *22*, 485501.

(15) Lin, T. C.; Huang, B. R. Temperature Effect on Hydrogen Response for Cracked Carbon Nanotube/nickel (CNT/Ni) Composite Film with Horizontally Aligned Carbon Nanotubes. *Sens. Actuators, B* **2013**, *185*, 548−852.

(16) Jung, D.; Han, M.; Lee, G. S. Gas Sensor Using a Multi-walled Carbon Nanotube Sheet to Detect Hydrogen Molecules. *Sens. Actuators, A* **2014**, *211*, 51−54.

(17) Cho, W.-S.; Moon, S.-I.; Lee, Y.-D.; Lee, Y.-H.; Park, J.-H.; Ju, B. K. Multiwall Carbon Nanotube Gas Sensor Fabricated Using Thermomechanical Structure. *IEEE Electron Device Lett.* **2005**, *26*, 498−500.

(18) Gupta, D.; Dutta, D.; Kumar, M.; Barman, P. B.; Sarkar, C. K.; Basu, S.; Hazra, S. K. A Low Temperature Hydrogen Sensor Based on Palladium Nanoparticles. *Sens. Actuators, B* **2014**, *196*, 215−222.

(19) Cui, S.; Pu, H.; Mattson, E. C.; Lu, G.; Mao, S.; Weinert, M.; Hirschmugl, C. J.; Gajdardziska-Josifovska, M.; Chen, J. Ag Nanocrystal as a Promoter for Carbon Nanotube-based Room-temperature Gas Sensors. *Nanoscale* **2012**, *4*, 5887−5894.

(20) Randeniya, L. K.; Martin, P. J.; Bendavid, A. Detection of Hydrogen Using Multi-walled Carbon-nanotube Yarns Coated with Nanocrystalline Pd and Pd/Pt Layered Structure. *Carbon* **2012**, *50*, 1786−1792.

(21) Santangelo, S.; Faggio, G.; Messina, G.; Fazio, E.; Neri, F.; Neri, G. On the Hydrogen Sensing Mechanism of Pt/TiO_2/CNTs Based Devices. *Sens. Actuators, B* **2013**, *178*, 473−484.

(22) Espinosa, E. H.; Ionescu, R.; Chambon, B.; Bedis, C.; Sotter, E.; Bittencourt, C.; Felten, A.; Pireaux, J.-J.; Correig, X.; Llobet, E. Hybrid Metal Oxide and Multiwall Carbon Nanotube Films for Low Temperature Gas Sensing. *Sens. Actuators, B* **2007**, *127*, 137−142.

(23) Espinosa, E. H.; Ionescu, R.; Bittencourt, C.; Felten, A.; Erni, R.; Tendeloo, G. V.; Pireaux, J.-J.; Llobet, E. Metal-decorated Multi-wall Carbon Nanotubes for Low Temperature Gas Sensing. *Thin Solid Films* **2007**, *515*, 8322−8327.

(24) Shim, J. Y.; Lee, J. D.; Jin, J. M.; Cheong, H. Comparison of Pd, Pt and Pt/Pd as Catalysts for Hydrogen Sensor Films. *J. Korean Phys. Soc.* **2009**, *55*, 2693−2696.

(25) Samerjai, T.; Tamaekong, N.; Liewhiran, C.; Wisitsoraat, A.; Tuantranont, A.; Phanichphant, S. Selectivity Towards H_2 Gas by

DOI: 10.1021/am506578j
ACS Appl. Mater. Interfaces 2015, 7, 3050−3057

Flame-made Pt-loaded WO3 Sensing Films. *Sens. Actuators, B* **2011**, *157*, 290−297.
(26) Tsukada, K.; Kiwa, T.; Yamaguchi, Y.; Migitaka, S.; Goto, Y.; Yokosawa, K. A Study of Fast Response Characteristics for Hydrogen Sensing with Platinum FET Sensor. *Sens. Actuators, B* **2006**, *114*, 158−163.
(27) Song, J. T.; Iwasaki, T.; Hatano, M. Pt Co-catalyst Effect on Photoelectrochemical Properties of 3C-SiC Photo-anode. *Jpn. J. Appl. Phys.* **2014**, *53*, 05FZ04.
(28) Liu, R.; King, H.; Lin, J.; Shen, F.; Cui, Z.; Zhang, T. Fabrication of Platinum-decorated single-walled Carbon Nanotube Based Hydrogen Sensors by Aerosol Jet Printing. *Nanotechnology* **2012**, *23*, 505301.
(29) Kumar, M. K.; Ramaprabhu, S. Nanostructured Pt Functionalized Multiwalled Carbon Nanotube Based Hydrogen Sensor. *J. Phys. Chem. B* **2006**, *110*, 11291−11298.
(30) Zhang, M.; Fang, S.; Zakhidov, A. A.; Lee, S. B.; Aliev, A. E.; Williams, C. D.; Atkinson, D. R.; Baughman, R. H. Strong, Transparent, Multifunctional, Carbon Nanotube Sheets. *Science* **2005**, *309*, 1215−1219.
(31) Jiang, K.; Wang, J.; Li, Q.; Liu, L.; Liu, C.; Fan, S. Superaligned Carbon Nanotube Arrays, Films, and Yarns: a Road to Applications. *Adv. Mater.* **2011**, *12*, 1154−1161.
(32) Jung, D.; Yoon, Y.; Lee, G. S. Hydrogen Sensing Characteristics of Carbon-nanotube Sheet Decorated with Manganese Oxides. *Chem. Phys. Lett.* **2014**, *122*, 281−284.
(33) Jung, D.; Lee, K. H.; Kim, D.; Overzet, L. J.; Lee, G. S. A Gas Sensor Using a Multi-walled Carbon Nanotube Sheet to Detect Oxygen Molecules. *J. Nanosci. Nanotechnol.* **2013**, *13*, 8275−8279.
(34) Han, M.; Jung, D.; Lee, G. S. Palladium-nanoparticle-coated Carbon Nanotube Gas Sensor. *Chem. Phys. Lett.* **2014**, *610−611*, 261−266.
(35) Lee, J.-H.; Kang, W.-S.; Najeeb, C. K.; Choi, B.-S.; Choi, S.-W.; Lee, H. J.; Lee, S. S.; Kim, J.-H. A Hydrogen Gas Sensor Using Single-walled Carbon Nanotube Langmuir-Blodgett Films Decorated with Palladium Nanoparticles. *Sens. Actuators, B* **2013**, *188*, 169−175.
(36) Helbling, T.; Pohle, R.; Durrer, L.; Stampfer, C.; Roman, C.; Jungen, A.; Fleischer, M.; Hierold, C. Sensing NO_2 with Individual Suspended Single-walled Carbon Nanotubes. *Sens. Actuators, B* **2008**, *132*, 491.
(37) Peng, Y.; Hu, Y.; Lu, W. Fabrication and Electrical Characterization of Multiwalled Carbon Nanotube-based Circuit at Room Temperature. *J. Nanomater.* **2011**, *2011*, 297534.
(38) Hierold, C.; Jungen, A.; Stampfer, C.; Helbling, T. Nano Electromechanical Sensors Based on Carbon Nanotubes. *Sens. Actuators, A* **2007**, *136*, 51−61.
(39) Lee, W. Y.; Weng, C. H.; Juang, Z. Y.; Lai, J. F.; Leou, K. C.; Tsai, C. H. Lateral Growth of Single-walled Carbon Nanotubes Across Electrodes and the Electrical Property Characterization. *Diamond Relat. Mater.* **2005**, *14*, 1852−1856.
(40) Li, Q.; Li, Y.; Zhang, X.; Chikkannanavar, S. B.; Zhao, Y.; Dangelewicz, A. M.; Zheng, L.; Doorn, S. K.; Jia, Q.; Peterson, D. E.; Arendt, P. N.; Zhu, Y. Structure-dependent Electrical Properties of Carbon Nanotube Fibers. *Adv. Mater.* **2007**, *19*, 3358−3363.
(41) Feng, C.; Liu, K.; Wu, J. S.; Liu, L.; Cheng, J.-S.; Zhang, Y.; Sun, Y.; Li, Q.; Fan, S.; Jiang, K. Flexible, Stretchable, Transparent Conducting Films Made from Superaligned Carbon Nanotubes. *Adv. Funct. Mater.* **2010**, *20*, 885−891.
(42) Jakubinek, M. B.; Johnson, M. B.; White, M. A.; Jayasinghe, C.; Le, G.; Cho, W.; Schulz, M. J.; Shanov, V. Thermal and Electrical Conductivity of Array-spun Multi-walled Carbon Nanotube Yarns. *Carbon* **2012**, *50*, 244−248.
(43) Jung, D.; Han, M.; Overzet, L. J.; Lee, G. S. Effect of Hydrogen Pretreatment on the Spin-Capability of a Multiwalled Carbon Nanotube Forest. *J. Vac. Sci. Technol., B* **2013**, *31*, 06FI02.
(44) Jung, D.; Kim, J. H.; Lee, K. H.; Overzet, L. J.; Lee, G. S. Effects of Pre-annealing of Fe Catalysts on Growth of Spin-capable Carbon Nanotubes. *Diamond Relat. Mater.* **2013**, *38*, 87−92.
(45) Jung, D.; Lee, K. H.; Overzet, L. J.; Lee, G. S. Effect of Carrier Gas on the Growth and Characteristics of Spin-capable Multiwalled Carbon Nanotubes. *IEEE Trans. Nanotechnol.* **2014**, *13*, 349−356.
(46) Kaniyoor, A.; Ramaprabhu, S. Hybrid Carbon Nanostructured Ensembles as Chemiresistive Hydrogen Sensors. *Carbon* **2011**, *49*, 227−236.
(47) Penza, M.; Rossi, R.; Alvisi, M.; Cassano, G.; Signore, M. A.; Serra, E.; Giorgi, R. Pt- and Pd-nanoclusters Functionalized Carbon Nanotubes Networked Films for Sub-ppm Gas Sensors. *Sens. Actuators, B* **2008**, *135*, 89−297.
(48) Kong, J.; Chapline, M. G.; Dai, H. Functionalized Carbon Nanotubes for Molecular Hydrogen Sensors. *Adv. Mater.* **2001**, *13*, 1384−1386.
(49) Shukla, S.; Zhang, P.; Cho, H. J.; Seal, S.; Ludwig, L. Room Temperature Hydrogen Response Kinetics of Nano-micro-integrated Doped tin Oxide Sensor. *Sens. Actuators, B* **2007**, *120*, 573−583.
(50) Lim, Z. H.; Chia, Z. X.; Kevin, M.; Wong, A. S. W.; Ho, G. W. A Facile Approach Towards ZnO Nanorods Conductive Textile for Room Temperature Multifunctional Sensors. *Sens. Actuators, B* **2010**, *151*, 121−126.
(51) Fasaki, I.; Suchea, M.; Mousdis, G.; Kiriakidis, G.; Kompitsas, M. The Effect of Au and Pt Nanoclusters on the Structural and Hydrogen Sensing Properties of SnO_2 Thin Films. *Thin Solid Films* **2009**, *518*, 1109−1113.
(52) Hung, N. L.; Ahn, E.; Park, S.; Jung, H.; Kim, H.; Hong, S.-K.; Kim, D.; Hwang, C. Synthesis and Hydrogen Gas Sensing Properties of ZnO Wirelike Thin Films. *J. Vac. Sci. Technol., A* **2009**, *27*, 1347:1−1347:5.
(53) Lupan, O.; Chai, G.; Chow, L. Novel Hydrogen Gas Sensor Based on Single ZnO Nanorod. *Microelectron. Eng.* **2008**, *85*, 2220−2225.
(54) Zhang, G.; Dang, L.; Li, L.; Wang, R.; Fu, H.; Shi, K. Design and Construction of Co_3O_4/PEI-CNTs Composite Exhibiting Fast Responding CO Sensor at Room Temperature. *CrystEngComm* **2013**, *15*, 4730−4738.
(55) Dang, L.; Zhang, G.; Kan, K.; Lin, Y.; Bai, F.; Jing, L.; Shen, P.; Li, L.; Shi, K. Heterostructured Co_3O_4/PEI-CNTs Composite: Fabrication, Characterization and CO Gas Sensors at Room Temperature. *J. Mater. Chem. A* **2014**, *2*, 4558−4565.
(56) Hübert, T.; Boon-Brett, L.; Black, G.; Banach, U. Hydrogen Sensors-A review. *Sens. Actuators, B* **2011**, *157*, 329−352.
(57) Aroutiounian, V. Hydrogen Detectors. *Int. Sci. J. Altern. Energy Ecol.* **2005**, *3*, 21−31.
(58) Jung, D.; Han, M.; Lee, G. S. Gas Sensing Properties of Multi-walled Carbon-nanotube Sheet Coated with NiO. *Carbon* **2014**, *78*, 156−163.
(59) Gu, H.; Wang, Z.; Hu, Y. Hydrogen Gas Sensors Based on Semiconductor Oxide Nanostructures. *Sensors* **2012**, *12*, 5517−5550.
(60) Penza, M.; Rossi, R.; Alvisi, M.; Cassanoa, G.; Serra, E. Functional Characterization of Carbon Nanotube Networked Films Functionalized with Tuned Loading of Au Nanoclusters for Gas Sensing Applications. *Sens. Actuators, B* **2009**, *146*, 176−184.
(61) Jung, D.; Lee, K. H.; Kim, D.; Burk, D.; Overzet, L. J.; Lee, G. S. Highly Conductive Flexible Multi-walled Carbon Nanotube Sheet Films for Transparent Touch Screen. *Jpn. J. Appl. Phys.* **2013**, *52*, 03BC03.
(62) Jung, D.; Han, M.; Lee, G. S. Flexible Transparent Conductive Heaters Using Multi-walled Carbon Nanotube Sheet. *J. Vac. Sci. Technol., B* **2014**, *32*, 04E105.
(63) Rothschild, A.; Komem, Y. The Effect of Grain Size on the Sensitivity of Nanocrystalline Metal-oxide Gas Sensors. *J. Appl. Phys.* **2004**, *95*, 6374−6380.
(64) Quang, N. H.; Trinh, M. V.; Lee, B.-H.; Huh, J.-S. Effect of NH_3 Gas on the Electrical Properties of Single-walled Carbon Nanotube Bundles. *Sens. Actuators, B* **2006**, *113*, 341−346.
(65) Nguyen, H.-Q.; Huh, J.-S. Behavior of Single-walled Carbon Nanotube-based Gas Sensor at Various Temperature of Treatment and Operation. *Sens. Actuators, B* **2006**, *117*, 426−430.

DOI: 10.1021/am506578j
ACS Appl. Mater. Interfaces 2015, 7, 3050−3057

(66) Nguyen, L. Q.; Phan, P. Q.; Duong, H. N.; Nguyen, C. D.; Nguyen, L. H. Enhancement of NH_3 Gas Sensitivity at Room Temperature by Carbon Nanotube-based Sensor Coated with Co Nanoparticles. *Sensors* **2013**, *13*, 1754−1762.
(67) Rajaputra, S.; Mangu, R.; Clore, P.; Qian, D.; Andrews, R.; Singh, V. P. Multi-walled Carbon Nanotube Arrays for Gas Sensing Applications. *Nanotechnology* **2008**, *19*, 345502.
(68) Snow, E. S.; Perkins, F. K.; Robinson, J. A. Chemical Vapor Detection Using Single-walled Carbon Nanotube. *Chem. Soc. Rev.* **2006**, *35*, 790−798.
(69) Sayago, I.; Santos, H.; Horrillo, M. C.; Aleixandre, M.; Fernandez, M. J.; Terrado, E.; Tacchini, I.; Aroz, R.; Maser, W. K.; Benito, A. M.; Martinez, M. T.; Gutierrez, J.; Munoz, E. Carbon Nanotube Networks as Gas Sensors for NO_2 Detection. *Talanta* **2008**, *77*, 758−764.
(70) Chen, W.-P.; Zhao, Z.-G.; Liu, X.-W.; Zhang, Z.-X.; Suo, C.-G. A Capacitive Humidity Sensor Based on Multi-walled Carbon Nanotubes (MWCNT). *Sensors* **2009**, *9*, 7431−744.

DOI: 10.1021/am506578j
ACS Appl. Mater. Interfaces 2015, 7, 3050−3057